

## Transmission-ion-channeling studies of the silicon (111) monohydride surface

W. R. Wampler

*Sandia National Laboratories, Albuquerque, New Mexico 87185*

(Received 12 April 1996; revised manuscript received 23 December 1996)

Transmission ion channeling was used to examine the atomic position of deuterium on the silicon (111) monohydride surface. A 2-MeV  $^4\text{He}^+$ -ion beam was used to elastically recoil deuterium from the beam-exit surface of a thin silicon crystal. The yield of recoiled deuterium was measured versus angle between the analysis beam and the channeling axis near the  $\langle 111 \rangle$ ,  $\langle 110 \rangle$ , and  $\langle 100 \rangle$  axes. The location of the surface deuterium relative to the silicon lattice was examined by comparing the measured yields with computer simulations of ion channeling. Channeling measurements were consistent with approximately half of the deuterium occupying a site close to the site predicted by *ab initio* calculations of the structure for the Si(111)  $1 \times 1$  monohydride surface, with the remaining deuterium being disordered or displaced from the predicted site. [S0163-1829(97)02616-7]

### I. INTRODUCTION

Hydrogen-terminated silicon surfaces have been intensively studied because of their importance for fabrication of semiconductor devices. Termination of dangling silicon bonds with hydrogen greatly reduces chemical reactivity of the surface, which helps maintain clean surfaces during processing. In addition, surface hydrogen strongly influences chemical vapor deposition and molecular-beam-epitaxial growth. Hydrogen termination of dangling bonds at surfaces and interfaces also strongly affects electronic properties. The large free energy associated with unterminated bonds on surface silicon atoms causes the surface to reconfigure to reduce the number of dangling bonds. The Si(100)  $2 \times 1$  dimer structure and the Si(111)  $7 \times 7$  structure are well-known examples. Hydrogen termination drastically alters the surface free energy, and thus also affects surface reconstruction. The influence of hydrogen termination on the structure of silicon surfaces has been investigated using low energy electron diffraction (LEED),<sup>1,2</sup> scanning tunneling microscopy (STM),<sup>3-6</sup> atomic force microscopy<sup>7</sup> and ion scattering.<sup>8</sup> These studies show that for the monohydride configuration, in which one hydrogen atom is attached to each surface silicon atom, the (100) surface retains the  $2 \times 1$  dimer structure of the unterminated surface. However, the surface silicon atoms on the (111) monohydride are close to their bulk lattice positions in contrast to the  $7 \times 7$  reconstruction of the unterminated (111) surface. Previous studies have shown that Si(111)  $1 \times 1$  monohydride terminated surfaces with very few structural imperfections can be prepared chemically using a solution of  $\text{NH}_4\text{F}$ ,<sup>3</sup> and by exposure of Si(111)  $7 \times 7$  surfaces at a temperature of 400 °C to atomic hydrogen.<sup>4</sup>

Several *ab initio* calculations of the Si(111)  $1 \times 1$  monohydride surface structure have been reported<sup>9-14</sup> which are in good agreement with each other, and which agree with observed Si-atom positions. These calculations predict that the hydrogen is located directly above the silicon atom to which it is bound with a bond length of  $1.53 \pm 0.01$  Å, close to the Si-H bond length of 1.48 Å in the silane molecule. However, there has been no quantitative experimental determination of the atomic position of hydrogen on the Si(111)  $1 \times 1$  monohydride surface, to our knowledge. Quantitative analysis of

LEED intensities<sup>2</sup> and medium-energy ion scattering<sup>8</sup> have been used to determine the atomic position of the surface silicon atoms, but not the hydrogen, on the Si(111)  $1 \times 1$  monohydride surface.

In a previous study,<sup>15</sup> the atomic position of deuterium on a Si(100)  $2 \times 1$  monohydride surface was determined by transmission ion channeling. Here we use transmission ion channeling to examine the atomic position of deuterium on a Si(111)  $1 \times 1$  monohydride surface [henceforth denoted H/Si(111)  $1 \times 1$ ] prepared by dosing with atomic deuterium. In Sec. II, the equipment and methods used to prepare and characterize the samples and to make the channeling measurements are described. In Sec. III, results from channeling measurements near the  $\langle 111 \rangle$ ,  $\langle 110 \rangle$ , and  $\langle 100 \rangle$  axes are presented. In Sec. IV, computer simulations of channeling are compared with channeling measurements to determine the atomic position of the deuterium.

### II. EXPERIMENTAL METHOD

#### A. Sample preparation and characterization

The thin silicon crystals used in this study were prepared from silicon-on-insulator wafers produced by a bond and etch-back process<sup>16</sup> which gave a high-quality (111) silicon layer 0.4  $\mu\text{m}$  thick with a resistivity of 1000  $\Omega$  cm on top of an  $\text{SiO}_2$  layer 1  $\mu\text{m}$  thick on a 525- $\mu\text{m}$ -thick (100) silicon wafer substrate.

The samples were etched in 4 M KOH solution at 80 °C to remove the substrate over a region about 3 mm in diameter at the center of sample. During etching, the front surface of the thin (111) silicon layer was protected a 0.25- $\mu\text{m}$ -thick layer of  $\text{Si}_3\text{N}_4$ , and the buried  $\text{SiO}_2$  layer provided an etch stop barrier between the thin (111) silicon layer and the substrate. Following the KOH etch, the  $\text{SiO}_2$  and  $\text{Si}_3\text{N}_4$  layers were removed in hydrofluoric acid. The above process yielded Si(111) crystals 0.4  $\mu\text{m}$  thick of high purity and the crystalline perfection required for transmission channeling experiments, supported by thicker surrounding substrate material by which samples could be handled during cleaning and mounting.

The method employed to prepare a well-ordered monohydride-terminated surface was to prepare a clean flat

surface with a thin oxide by wet chemistry,<sup>3</sup> thermally desorb the oxide in UHV to produce a Si(111)  $7\times 7$  surface,<sup>17</sup> and then dose with atomic hydrogen at 400 °C to give a H/Si(111)  $1\times 1$  surface.<sup>4</sup> Since the quality of the surface depends on how it was prepared, the following gives details of the procedure used.

After removal of the SiO<sub>2</sub> and Si<sub>3</sub>N<sub>4</sub> layers, the samples were placed in H<sub>2</sub>O:HCl:H<sub>2</sub>O<sub>2</sub> (5:1:1) at 80 °C for 10 min to produce a clean thin chemical oxide. The samples were then placed in a 40% solution of NH<sub>4</sub>F, which removes the oxide and leaves a clean atomically flat well-ordered H/Si(111)  $1\times 1$  surface.<sup>3</sup> The samples were then chemically oxidized a second time. After this final oxidation and between each step in the above chemical treatment, the samples were rinsed in deionized water. After the final rinse the samples were mounted on a molybdenum holder, and transferred through a load lock onto a channeling goniometer in an ion pumped UHV analysis chamber with a base pressure below  $2\times 10^{-10}$  Torr.

The sample and sample holder were radiatively heated to 400 °C by a tungsten filament near the holder. The sample temperature was held at 400 °C for 10 min to desorb hydrocarbons. A heat lamp focused on the sample was then turned on for 2 min to raise the sample temperature above 800 °C where the surface oxide desorbs.<sup>17</sup> The sample was then cooled back to 400 °C, where it was exposed to atomic deuterium (D) produced by thermal dissociation of D<sub>2</sub> gas on a tungsten filament near the sample. After dosing with atomic D, the sample was cooled to room temperature where all further measurements were done.

Owman and Mårtensson<sup>4(a)</sup> used STM to examine the structure of the H/Si(111)  $1\times 1$  surface produced by exposing a Si(111)  $7\times 7$  surface to atomic H. Their atomic H was also produced by thermal dissociation of molecular H<sub>2</sub> on a tungsten filament, and they reported their doses in units L of molecular H<sub>2</sub> exposure. They found that, for doses of 50 L, the silicon adatoms of the  $7\times 7$  surface clustered into islands on a surface with much of the stacking faulted regions of the original  $7\times 7$  surface remaining. Higher doses reduced the area of stacking faults and the number of atoms in the islands. The stacking faults present after low H doses produced streaks in the LEED pattern between the  $1\times 1$  spots which became visible when the faulted region exceeded 10% of the total area. In our experiments we measured the surface coverage of D and observed the LEED pattern after various doses of atomic D at 400 °C. The D coverage was observed to saturate at 1 ML for doses above about 200 L. Doses of 2400 and 4800 L gave sharp  $1\times 1$  LEED patterns with a low diffuse background and no streaks as shown in Fig. 1. This  $1\times 1$  LEED pattern is the same as that observed on samples chemically H terminated in NH<sub>4</sub>F which is known to produce a well-ordered H/Si(111)  $1\times 1$  surface.<sup>3</sup> Figure 1 also shows the Si(111)  $7\times 7$  LEED pattern observed after heating the sample above 800 °C but prior to dosing with atomic D.<sup>18</sup> These LEED results show that an ordered H/Si(111)  $1\times 1$  surface structure was produced by the atomic D dosing.

Contamination of the surface from residual gas in the vacuum system was avoided by minimizing the time between desorption of the oxide and formation of the monohydride, since oxide and hydrogen termination both greatly reduce the chemical reactivity of the surface. Auger electron

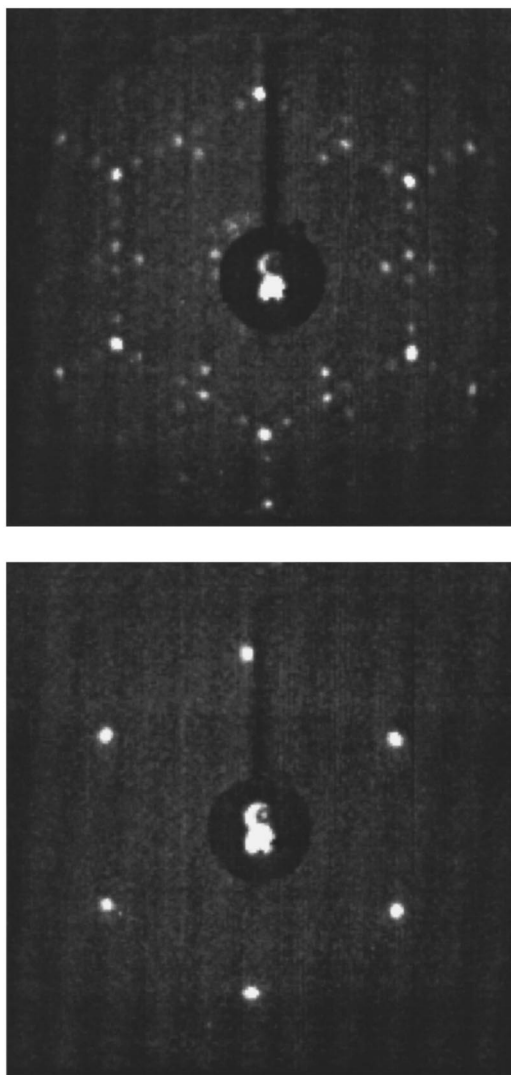


FIG. 1. LEED images taken at 60 eV on thin Si(111) crystals used for transmission channeling studies for the  $7\times 7$  surface after heating above 800 °C (above), and for the H/Si(111)  $1\times 1$  surface produced by exposing the  $7\times 7$  surface at 400 °C to atomic D (below).

spectroscopy (AES) showed surface impurities to be below the limit of detection which is about 0.03 ML for carbon and oxygen. Desorption of D during AES analysis was avoided by keeping the electron-beam current below 1  $\mu$ A. The AES and LEED measurements were done on the ion-beam exit surface of the samples.

Since the thin crystal region must be flat for channeling experiments, its flatness was checked by reflecting a low-power HeNe laser beam from the thin region of the sample. This technique showed the thin region of the sample was flat within 0.05° both before and after dosing with atomic D. Results from AES, LEED, and laser reflection examinations were the same before and after the channeling measurements, showing that the composition, structure, and flatness of the sample did not change during the channeling measurements.

### B. Ion-beam analysis and transmission-ion-channeling measurements

Ion channeling has been used extensively to study the location of foreign atoms within a host crystal lattice.<sup>19</sup> When an analysis beam of energetic ions is directed onto a crystal along a high-symmetry direction, the ions are deflected away from the rows or planes of lattice atoms towards the center of the open channels. After passing a short distance ( $\sim 100$  nm) through the lattice, an equilibrium distribution of ion flux within the channel is established which has maxima at the center of the channel and minima along the rows of lattice atoms. The flux distribution within the channel depends strongly on the angle between the incident ion beam and the channel direction, or channeling angle. The scattering yield from foreign atoms is proportional to the ion flux at the location of the foreign atom, and hence depends on the channeling angle and on the location of the foreign atom within the channel. Measurements of scattering yield versus channel angle, i.e., channeling scans, about the major crystallographic directions are compared with computer simulations of channeling scans to determine the lattice coordinates of the foreign atoms.

If the target crystal is thin enough for the analysis beam to pass through it, the position of foreign atoms on the beam exit or downstream surface can also be determined by this method.<sup>15,19–21</sup> Such experiments require a free-standing thin crystal only a few hundred nm thick. The flux distribution of the analysis beam within the channels at the exit surface is essentially the same as in the bulk crystal, and is not altered significantly by surface reconstruction. Thus the measured scattering yields depend on the position of the foreign atoms on the surface relative to the bulk crystal lattice in the same way as it would for foreign atoms within the lattice.

The channeling experiments in this investigation were done by measuring the yield of D elastically recoiled from the beam exit side of the sample. The sample was oriented such that the beam exit surface was the original outer surface of the SOI wafer. D was removed from the beam entry surface by sputtering so that yields of scattered D measured during the channeling experiments were only from D on the beam exit surface.

The analysis beam used for the channeling experiments was  $^4\text{He}^+$ , with an energy near 2 MeV, and an angular divergence of  $0.03^\circ$ . The size of the analysis beam spot at the sample was  $1 \times 1 \text{ mm}^2$ . A bakable silicon surface barrier detector with standard nuclear electronics for pulse-height analysis was used to collect energy spectra of scattered and recoiled particles. One detector for Rutherford backscattering (RBS), faced the beam entry side of the sample, and analyzed  $^4\text{He}$  backscattered from silicon atoms through an angle of  $150^\circ$ . The ratio of the yield on axis to the yield off axis ( $\chi_{\min}$ ) is a measure of the crystalline perfection of the sample. The values of  $\chi_{\min}=0.055$ ,  $0.048$ , and  $0.077$  for the  $\langle 111 \rangle$ ,  $\langle 110 \rangle$ , and  $\langle 100 \rangle$  axes, respectively (Fig. 2), are close to the  $\chi_{\min}$  measured in bulk silicon.<sup>22</sup> This shows that for purposes of channeling, the thin crystals used in our transmission channeling studies were equivalent to high-quality bulk silicon wafers.

A second detector, which faced the beam exit side of the sample and was coaxial with the analysis beam, analyzed D

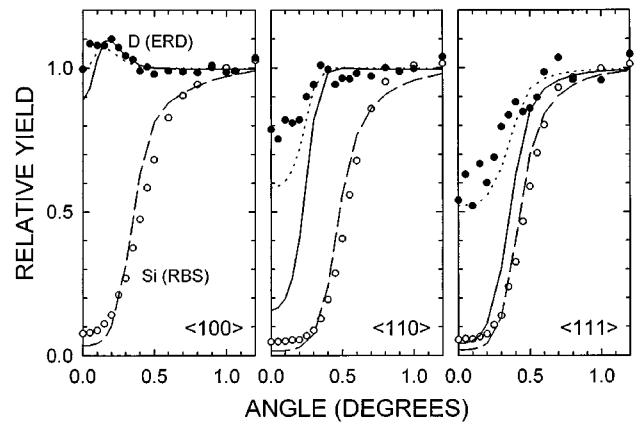


FIG. 2. Data from transmission-channeling measurements. Solid circles show the yield of recoiled D, open circles show the yield of He backscattered from silicon. Also shown are computer simulations for backscattered He (dashed curve) and recoiled D (solid curve) at the location predicted by *ab initio* calculations. The dotted curve shows a simulation for the case where 50% of the D is disordered and 50% is directly above the surface silicon atoms with a Si-D bond length of 1.43 Å.

and H elastically recoiled from the sample by the  $^4\text{He}$  beam. A  $12\text{-}\mu\text{m}$ -thick aluminum range foil in front of this detector stopped the scattered He, but still transmitted recoiled H and D. The central portion of the elastic recoil detector was covered by a blocking disk thick enough to stop all particles, to prevent H and D on the range foil from being recoiled into the detector. The detector configuration allowed particles recoiled from the sample through angles between  $4.9^\circ$  and  $11.9^\circ$  to enter the detector.

Counts from recoiled H and D can be distinguished by their different energies, due to the factor of two mass difference and the kinematics of elastic scattering. Elastic recoil detection (ERD) thus allows the areal densities of H and D on the sample to be independently measured. Samples cleaned and dosed with atomic D as described above had only D with no detectable H. Since the differential scattering cross sections for H or D recoiled by  $^4\text{He}$  are known,<sup>23–25</sup> the areal density of H or D on the sample can be absolutely determined from the measured ERD yields. The absolute accuracy of values for H and D coverage determined from ERD yields is estimated to be  $\pm 6\%$  for D and  $\pm 20\%$  for H, due mainly to uncertainties in the scattering cross sections. The relative accuracy, for comparisons between measured values, is mainly determined by counting statistics.

A narrow resonance in the cross section for D recoiled by  $^4\text{He}$  at 2.13 MeV (Ref. 25) was used to determine the D coverage on the beam entry and beam exit surfaces independently, as described in Ref. 15. The absence of a narrow resonance in the elastic-scattering cross section for H recoiled by  $^4\text{He}$  (Refs. 23 and 24) precluded the use of this technique for H, and only the sum of H coverages on the beam-entry and -exit surfaces could be measured.

The sample could be tilted up to  $60^\circ$  from normal to the beam without obstructing line of sight to the ERD or RBS detectors or the analysis beam, thus allowing channeling measurements along the  $\langle 111 \rangle$ ,  $\langle 110 \rangle$ , and  $\langle 100 \rangle$  axes.

### III. CHANNELING RESULTS

Channeling data were taken on two Si(111) samples. The first sample was prepared as described in Sec. II A with a 2400-L exposure giving a  $1 \times 1$  LEED pattern. Resonance ERD depth profiling showed there was  $7.4 \text{ D/nm}^2$  on the beam-entry side and  $7.3 \text{ D/nm}^2$  on the beam-exit side of the sample after dosing. D coverage on the beam-entry surface was reduced to  $0.5 \text{ D/nm}^2$  by sputtering, and channeling scans were measured. This sample was then heated with the heat lamp to desorb the D, after which the total (both beam-entry and -exit surfaces) coverages of H and D were  $<1 \text{ H/nm}^2$  and  $<0.2 \text{ D/nm}^2$ , respectively, and a  $7 \times 7$  LEED pattern was observed. The same sample was then exposed again to atomic D to the higher dose of 4800 L giving a  $1 \times 1$  LEED pattern. D was sputtered from the beam-entry surface, and channeling scans were again measured, after which the coverage of D on the beam-exit surface was  $8.5 \text{ D/nm}^2$ .

A second sample was prepared as described in Sec. II A with a dose of 4800 L. D was sputtered from the beam-entry surface, and channeling scans were measured. The coverage of D on the beam-exit surface of this sample was  $7.6 \text{ D/nm}^2$ . The coverage of D on all surfaces after dosing with atomic D to produce the H/Si(111)  $1 \times 1$  surface was very close to the value of  $7.8 \text{ D/nm}^2$ , corresponding to one D per surface Si atom, consistent with the coverage for the monohydride configuration.

Channeling scans were measured for the  $\langle 111 \rangle$ ,  $\langle 110 \rangle$ , and  $\langle 100 \rangle$  axes. ERD and RBS spectra were recorded at several angles between  $0^\circ$  and  $1.2^\circ$  from the axis. To average out planar channeling effects, the spectrum for each angle was the sum of measurements at 50 points around a circle of constant angle from the axis. The channeling data were taken with an analysis beam energy of 2 MeV. The beam energy at the exit surface is lower than 2 MeV due to energy loss passing through the sample. The beam energy was chosen so that small variations in the beam energy at the exit surface due to channeling effects would not cause significant changes in the ERD scattering cross section.

Analysis beam doses to the sample were kept small ( $\sim 12 \mu\text{C}$  per channeling scan) to minimize effects of the analysis beam on the sample. Tests were made to check whether exposure to the analysis beam caused any degradation of the sample, either through displacement of the silicon atoms, which would have increased  $\chi_{\text{min}}$  or through changes in the configuration or coverage of surface D, which would have changed the ERD scans. In most cases each channeling scan was measured twice to insure reproducibility. These tests showed there were no significant analysis beam induced changes in the samples.

Results from the two sets of channeling measurements on the first sample and the one set on the second sample were all the same within the statistical accuracy of the measurements. Figure 2 shows the data from these three sets of channeling measurements averaged together for each axis. The main features of the data can be qualitatively summarized as follows. The ERD yield had a dip on the  $\langle 111 \rangle$  axis to about 55% of the off-axis value. The ERD yield had a dip on the  $\langle 110 \rangle$  axis to about 80% of the off-axis value. On the  $\langle 100 \rangle$  axis the ERD yield was about the same on-axis as off-axis, but had a 10% peak about  $0.2^\circ$  off-axis.

### IV. COMPUTER SIMULATIONS OF CHANNELING AND D POSITION

The atomic position of the D on the H/Si(111)  $1 \times 1$  surface was examined by comparing the measured channeling data with computer simulations of channeling. The simulations were done using a computer model developed by Bech Nielsen,<sup>26</sup> which is based on the continuum model for channeling and which includes dechanneling and vibrational motion of the D and Si atoms. As a starting point for this discussion we calculate the channeling scans for hydrogen at the location predicted by the *ab initio* calculations<sup>9-14</sup> of the atomic structure of the H/Si(111)  $1 \times 1$  surface. These *ab initio* calculations are in good agreement with each other and predict a Si-H bond length of  $1.53 \text{ \AA}$  in the tetrahedral bond direction, i.e., normal to the (111) surface. Relaxation of the surface silicon atoms from their bulk lattice position also affects the H location relative to the Si lattice. Medium-energy ion scattering<sup>8</sup> and quantitative analysis of LEED intensities<sup>2</sup> show that the outermost Si atom layer on the H/Si(111)  $1 \times 1$  surface is displaced inward  $0.08 \text{ \AA}$  from the unrelaxed or bulk lattice position. Thus the theoretically predicted H-atom location is  $1.45 \text{ \AA}$  from the unrelaxed lattice site of the Si atom to which it is bound. Thermal and zero-point vibrational motion of the H also influences the yield of recoiled H. Vibrational frequencies of H on the H/Si(111)  $1 \times 1$  surface have been measured by electron-energy-loss spectroscopy which gives  $2084$  and  $636 \text{ cm}^{-1}$  for the Si-H stretching and bending modes respectively.<sup>27</sup> For a harmonic oscillator the vibrational frequencies for Si-D are lower than those of Si-H by a factor of approximately 0.707 because of the mass difference between H and D. A quantum harmonic oscillator with these frequencies has vibrational amplitudes for Si-D at 300 K of  $0.2 \text{ \AA}$  for the bending mode and  $0.1 \text{ \AA}$  for the stretching mode, mostly due to zero-point motion. The channeling simulation also includes dechanneling of the analysis beam due to vibrational motion of the bulk silicon lattice. The two-dimensional rms vibrational amplitude of the Si was estimated to be  $0.1 \text{ \AA}$  from the Si lattice Debye temperature.<sup>28</sup> Figure 2 shows calculated channeling scans for the theoretically predicted H location and vibrational amplitudes discussed above. For He backscattered from silicon, the calculated and measured curves are in good agreement. The calculated channeling scans for the recoiled D agree qualitatively with the data in the sense that channeling dips are seen for the  $\langle 111 \rangle$  and  $\langle 110 \rangle$  axes, and a peak slightly off-axis is seen for the  $\langle 100 \rangle$  axis. However, the measured channeling dips at the  $\langle 111 \rangle$  and  $\langle 110 \rangle$  axes are not as deep as predicted. This difference between measured and calculated channeling dips cannot be reconciled by adjusting the Si-D bond length, since displacements of the D in the  $\langle 111 \rangle$  direction do not affect the position of the D within the  $\langle 111 \rangle$  axial channel and hence have no effect on the calculated channeling dip for the  $\langle 111 \rangle$  axis. The difference between measured and calculated channeling dips also cannot be due to effects of analysis beam divergence or to dechanneling by curvature of the thin silicon crystal or by defects in the Si crystal, since such effects would also reduce the depth of the Si RBS channeling dips contrary to observation. The

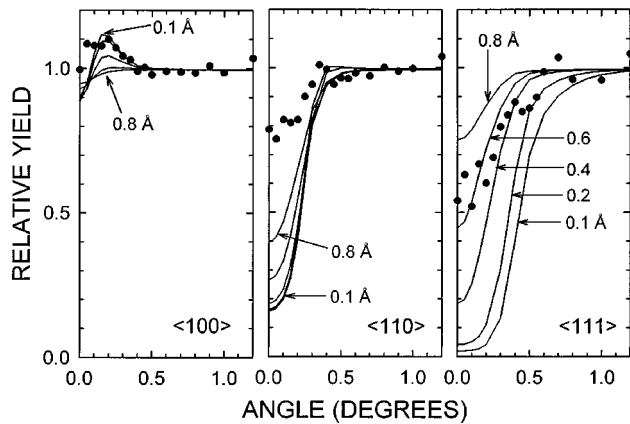


FIG. 3. Simulated channeling scans for various D vibrational amplitudes about the theoretically predicted location 1.53 Å above the surface silicon atoms.

observed difference between measured and calculated yields for recoiled D at the  $\langle 111 \rangle$  axis leads to the conclusion that a significant fraction of the D is not in line with the rows of Si atoms, but is displaced laterally, i.e., parallel to the surface, from the position expected for the ordered H/Si(111)  $1 \times 1$  surface.

In the following discussion we examine whether these displacements might be due to a larger than expected thermal vibrational amplitude or to static disorder. Thermal vibrations are included in the computer simulation by assuming a spherically symmetric Gaussian probability distribution for the D about its equilibrium position.<sup>26</sup> Figure 3 shows the effect on the calculated channeling scans, of varying the D vibrational amplitude from 0.1 to 0.8 Å. For the  $\langle 111 \rangle$  axis the channeling dip becomes shallower as the D vibrational amplitude increases. However, no single value of vibrational amplitude gives the observed depth for both the  $\langle 111 \rangle$  and  $\langle 110 \rangle$  channeling dips. Increasing the vibrational amplitude also decreases the width of dip at the  $\langle 111 \rangle$  axis. A vibrational amplitude of 0.3 Å gives the closest agreement between the widths of the calculated and measured channeling dips at the  $\langle 111 \rangle$  axis.

Next we examined whether static tilting of the Si-D bond away from the surface normal direction can account for the observed channeling results. Such a tilting of the Si-D bond direction would not affect LEED patterns, and might also be difficult to detect by STM. In these simulations the surface Si atoms were fixed at the location described above, and the Si-D bond length was held constant at 1.53 Å while displacement components along the directions of the second-to-first-layer Si-Si bonds were added to the Si-D bond direction. The three equivalent directions for such displacements were assumed to be equally probable. For this simulation the rms vibrational amplitude of the D was chosen to be 0.2 Å. These lateral displacements do not reproduce the observed channeling results. In particular, lateral displacements up to 0.68 Å (corresponding to tilt angles up to 26° from normal) produce little change in the channeling dip at the (110) axis, while lateral displacements greater than 0.5 Å give channeling results in qualitative disagreement with experiment for the (100) and (111) axes.

The effect on the channeling scans of varying the Si-D bond length was also examined. For this comparison the

Si-D bond direction was taken to be normal to the surface, and the rms vibrational amplitude of the D was chosen to be 0.2 Å. Displacements normal to the surface have no effect on the channeling dip at the  $\langle 111 \rangle$  axis, and little effect on the channeling dip at the  $\langle 110 \rangle$  axis. The strongest effect is on the channeling scan at the  $\langle 100 \rangle$  axis. Qualitative agreement between measured and calculated  $\langle 100 \rangle$  channeling scans is somewhat better for a bond length 0.1 Å, shorter than predicted, but significantly worse for bond lengths 0.1 Å or more longer than predicted by *ab initio* structure calculations.

Agreement between calculated and measured channeling scans can be significantly improved by assuming that only a fraction of the D is on the predicted site, and the remaining D is disordered, i.e., randomly distributed. The dotted curve in Fig. 2 shows the calculated channeling scans for the case where 50% of the D is disordered and 50% is directly above the surface Si atoms with a bond length of 1.43 Å, which is 0.1 Å shorter than predicted by *ab initio* calculations.

The fraction of D which was disordered did not significantly change when the atomic D dose used to prepare the monohydride surface was changed by a factor of 2. Disorder might result from residual defects in H/Si(111)  $1 \times 1$  surfaces prepared by dosing with atomic hydrogen, i.e., the islands, holes and stacking faults described by Owman and Mårtensson.<sup>4</sup> It may also be possible that the density of such defects differs between H- and D-terminated surfaces. If such surface defects are the cause of the observed D disorder, then our experiments show that these defects do not significantly change the D coverage from that of an ideal monohydride-terminated surface. The observed monolayer D coverage also shows that few silicon dihydride and trihydride units are present on the surface since these would increase the ratio of D/Si. The possibility that the apparent D disorder is related to residual surface defects could be tested by repeating the channeling measurements using H/Si(111)  $1 \times 1$  surfaces prepared by chemical termination using  $\text{NH}_4\text{F}$ , which have been shown to have very few defects.<sup>3,29</sup>

Another possible cause of the apparent D-disorder may be the presence of additional large amplitude vibrational modes of the D or of the surface silicon atoms. This could be tested by conducting channeling experiments at low temperatures to reduce lattice vibrations.

## V. SUMMARY

Si(111)  $1 \times 1$  monohydride surfaces were prepared by dosing Si(111)  $7 \times 7$  surfaces at 400 °C with atomic D. Three sets of measurements on two samples gave the same results. In each case LEED indicated a well-ordered  $1 \times 1$  structure, and measurement of the D coverage by ERD gave a 1:1 ratio of surface D to surface Si atoms, consistent with a monohydride-terminated surface. Channeling measurements were reproducible, and were consistent with approximately half of the D occupying a site close to the site predicted by *ab initio* calculations of the structure for the Si(111)  $1 \times 1$  monohydride surface, with the remaining D being disordered or displaced from the predicted site.

## ACKNOWLEDGMENT

This work was funded by the Office of Basic Energy Sciences, Division of Materials Science of the U.S. Department of Energy under Contract No. DE-AC04-94AL85000.

- <sup>1</sup>H. Ibach and J. E. Rowe, *Surf. Sci.* **43**, 481 (1974).
- <sup>2</sup>F. Jona, W. A. Thompson, and P. M. Marcus, *Phys. Rev. B* **52**, 8226 (1995).
- <sup>3</sup>G. S. Higashi, R. S. Becker, Y. J. Chabal, and A. J. Becker, *Appl. Phys. Lett.* **58**, 1656 (1991).
- <sup>4</sup>F. Owman and P. Mårtensson, (a) *Surf. Sci. Lett.* **303** L367 (1994); (b) *Surf. Sci.* **324**, 211 (1995).
- <sup>5</sup>J. J. Boland, *Surf. Sci.* **261**, 17 (1992).
- <sup>6</sup>J. J. Boland, *Adv. Phys.* **42**, 129 (1993).
- <sup>7</sup>M. Kageshima, H. Yamada, Y. Morita, H. Tokumoto, K. Nakayama, and A. Kawazu, *Jpn. J. Appl. Phys.* **32**, L1321 (1993).
- <sup>8</sup>M. Opel, R. J. Culbertson, and R. M. Tromp, *Appl. Phys. Lett.* **65**, 2344 (1994).
- <sup>9</sup>X. Blase, X. Zhu, and S. G. Louie, *Phys. Rev. B* **49**, 4973 (1994).
- <sup>10</sup>K. Hricovini, R. Günther, P. Thiry, A. Taleb-Ibrahimi, G. Indlekofer, J. E. Bonnet, P. Dumas, Y. Petrof, X. Blase, X. Zhu, S. G. Louie, Y. J. Chabal, and P. A. Thiry, *Phys. Rev. Lett.* **70**, 1992 (1993).
- <sup>11</sup>M. B. Nardelli, F. Finocchi, M. Palumbo, R. di Felice, C. M. Bertoni, F. Bernardini, and S. Ossicini, *Surf. Sci.* **269**, 879 (1992).
- <sup>12</sup>X. P. Li and D. Vanderbilt, *Phys. Rev. Lett.* **69**, 2543 (1992).
- <sup>13</sup>E. Kaxiras and J. D. Joannopoulos, *Phys. Rev. B* **37**, 8842 (1988).
- <sup>14</sup>K. M. Ho, M. L. Cohen, and S. Schlüter, *Phys. Rev. B* **15**, 3888 (1977).
- <sup>15</sup>W. R. Wampler, *Phys. Rev. B* **51**, 4998 (1995).
- <sup>16</sup>AcuThin™ SOI wafers were obtained from Hughes Danbury Optical Systems, Inc., 100 Wooster Heights Road, Danbury, CT 06810.
- <sup>17</sup>A. Ishizaka and Y. Shiraki, *J. Electrochem. Soc.* **133**, 666 (1986).
- <sup>18</sup>J. D. Levine, S. H. McFarlane, and P. Mark, *Phys. Rev. B* **16**, 5415 (1977).
- <sup>19</sup>I. Stensgaard and F. Jakobsen, *Phys. Rev. Lett.* **54**, 711 (1985).
- <sup>20</sup>K. Mortensen, F. Besenbacher, I. Stensgaard, and W. R. Wampler, *Surf. Sci.* **205**, 433 (1988).
- <sup>21</sup>F. Besenbacher, I. Stensgaard, and K. Mortensen, *Surf. Sci.* **191**, 288 (1987).
- <sup>22</sup>*Materials Analysis by Ion Channeling*, edited by L. C. Feldman, J. W. Mayer, and S. T. Picraux (Academic, New York, 1982).
- <sup>23</sup>E. Szilagy, F. Paszti, A. Manuaba, C. Hajdu, and E. Kotai, *Nucl. Instrum. Methods Phys. Res. Sect. B* **43**, 502 (1989).
- <sup>24</sup>J. E. E. Baglin, A. J. Kellock, M. A. Crockett, and A. H. Smith, *Nucl. Instrum. Methods Phys. Res. Sect. B* **64**, 469 (1992).
- <sup>25</sup>F. Besenbacher, I. Stensgaard, and P. Vase, *Nucl. Instrum. Methods Phys. Res. Sect. B* **15**, 459 (1986).
- <sup>26</sup>B. Bech Nielsen, *Phys. Rev. B* **37**, 6353 (1988).
- <sup>27</sup>P. Dumas and Y. J. Chabal, *J. Vac. Sci. Technol. A* **10**, 2160 (1992).
- <sup>28</sup>D. S. Gemmel, *Rev. Mod. Phys.* **46**, 129 (1974).
- <sup>29</sup>P. Jacob, Y. J. Chabal, K. Raghavachari, P. Dumas, and S. B. Christman, *Surf. Sci.* **285**, 251 (1993).